

an Unsteady MHD Free Convection Flow of a Casson Fluid past over an Oscillating Vertical Plate

DR. ANJAN KUMAR DEKA
Normal school, Sootea ,Biswanath ,Assam

ABSTRACT

The boundary layer flow of an unsteady MHD free convection heat and mass transfer flow of a viscous incompressible and electrically conducting Casson fluid over an oscillating vertical plate with Newtonian heating on the wall under the effects of chemical reaction and thermal radiation has been investigated in this chapter.. Casson fluid model is used to characterize the fluid behavior. The magnetic Reynolds number is considered to be so small that the induced magnetic field can be neglected. Exact solution of the governing equations is obtained in closed form by Laplace transform technique. The effects of the pertinent flow parameters on velocity, temperature and concentration field are presented graphically and discussed here .

Keywords: skin friction, magnetic field, heat transfer, mass transfer, porous medium .

1.INTRODUCTION

The analysis of boundary layer flow of viscous and non-Newtonian fluids has been the focus of extensive research by various scientists due to its importance in continuous casting, paper production, glass blowing, aerodynamic extrusion of plastic sheet, polymer extrusion and several others. Convective heat transfer plays an important role during the handling and processing of non-Newtonian fluid flows. Mechanics of non-Newtonian fluid flows present a special challenge to engineers, physicists, and mathematicians. Because of the complexity of these fluids, there is not a single constitutive equation which exhibits all properties of such non-Newtonian fluids. In the process, a number of non-Newtonian fluid models have been proposed. These simple fluid models have the shortcomings that render results that are not in accordance with the fluid flows in reality. The model predicts shear thinning and shear thickening behavior.

The second grade fluid model is the simplest subclass of viscoelastic fluids for which one can reasonably hope to obtain the analytic solution. Normal stress effects can be expressed in second grade fluid model, a special type of Rivlin–Ericksen fluids, but this model is incapable of representing shear thinning/thickening behavior (Aksoy et al. (2007)). The non-Newtonian fluids are mainly classified into three types, namely differential, rate, and integral. The simplest subclass of the rate type fluids is the Maxwell model which can predict the stress relaxation. This rheological model, also, excludes the complicated effects of shear dependent viscosity from any boundary layer analysis (Hayat et al. (2011)). There is another type of non-Newtonian fluid known as Casson fluid. Casson fluid exhibits yield stress. It is well known that Casson fluid is a shear thinning liquid which is assumed to have an infinite viscosity at zero rate of shear, a yield stress below which no flow occurs, and a zero viscosity at an infinite rate of shear, i.e., if a shear stress less than the yield stress is applied to the fluid, it behaves like a solid, whereas if a shear stress greater than yield stress is applied, it starts to move. In all these studies mentioned above, the Newtonian heating condition was neglected at the boundary..

2 .Mathematical Analysis :Let us consider the unsteady MHD natural convection flow with heat and mass transfer of a viscous, incompressible, electrically conducting, thermalradiative and chemically reactive Casson fluid over an oscillating vertical plate with Newtonian

heating on the wall. Coordinate system is chosen in such a way that x' -axis is considered along the plate in upward direction and y' -axis normal to plane of the plate in the fluid. Initially i.e., at time $t' \leq 0$, both the fluid and plate are at rest and are maintained at a uniform temperature T'_∞ . Also species concentration at the surface of the plate as well as at every point within the fluid is maintained at uniform concentration C'_∞ . At time $t' > 0$, the plate starts oscillation in its plane ($y = 0$) with velocity $V = UH(t)\cos \omega t \hat{i}$, where the constant U is the amplitude of the plate oscillations, $H(t)$ is the unit step function, \hat{i} is the unit vector in the vertical flow direction and ω is the frequency of the oscillation of the plate. The species concentration at the surface of the plate is raised to uniform species concentration C'_w and is maintained thereafter. Geometry of the problem is presented in Fig1. Since plate is of infinite extent in x' and z' directions and is electrically non-conducting, all physical quantities except pressure depend on y' and t' only. Also no applied or polarized voltages exist so the effect of polarization of

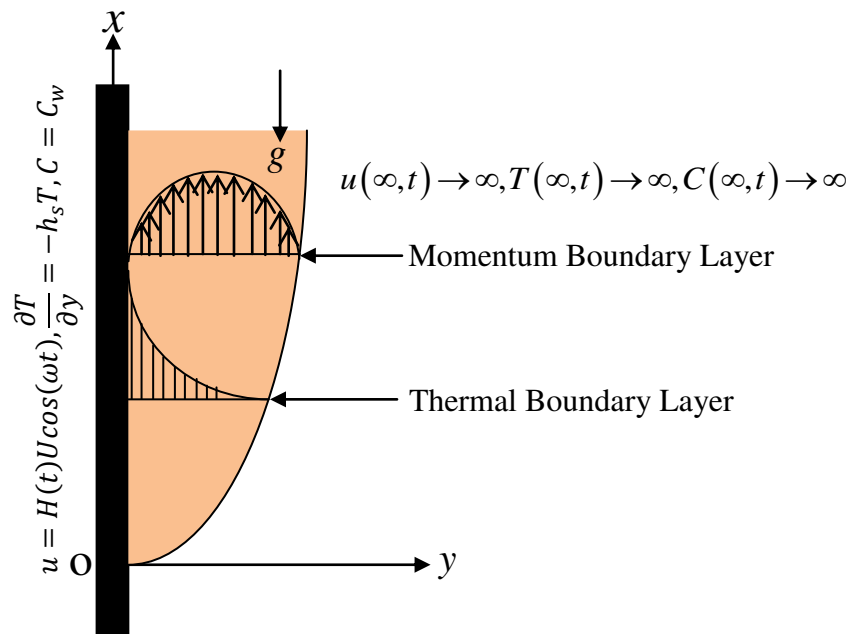


Fig.1: Geometry of the Problem

fluid is negligible. This corresponds to the case where no energy is added or extracted from the fluid by electrical means (1973). It is assumed that the induced magnetic field generated by fluid motion is negligible in comparison to the applied one. This assumption is justified because magnetic Reynolds number is very small for liquid metals and partially ionized fluids which are commonly used in industrial applications (1973). According to Newtonian heating, the heat transfer from the surface to the fluid is directly proportional to the T . In view of the above assumptions and taking into account the rheological equation for an incompressible and isotropic Casson fluid represented by Casson(1959) is

$$\tau = \tau_0 + \mu \alpha^*$$

Equivalently,

$$\tau_{ij} = \begin{cases} 2 \left(\mu_B + \frac{p_y}{\sqrt{2\pi}} \right) e_{ij}, \pi > \pi_c \\ 2 \left(\mu_B + \frac{p_y}{\sqrt{2\pi_c}} \right) e_{ij}, \pi < \pi_c \end{cases}$$

where τ, τ_0, μ and α^* are, respectively shear stress, Casson yield stress, dynamic viscosity and shear rate and $\pi = e_{ij}e_{ij}$ and e_{ij} is the (i, j)th component of deformation rate, π is the product of component of deformation rate with itself, π_c is a critical value of this product based on the non-Newtonian model, μ_B is the plastic dynamic viscosity of the non-Newtonian fluid, and p_y denote the yield stress of the fluid.

Keeping in view the assumptions made above, governing equations for the fully developed hydromagnetic natural convection flow with heat and mass transfer of an electrically conducting, viscous, incompressible, thermal radiative and chemically reactive Casson fluid over an oscillating vertical plate with Newtonian heating on the wall are

Conservation of momentum:

$$\frac{\partial u'}{\partial t'} = \nu \left(1 + \frac{1}{\alpha} \right) \frac{\partial^2 u'}{\partial y'^2} + g\beta(T' - T'_\infty) + g\beta'(C' - C'_\infty) \tag{2.1}$$

Conservation of energy:

$$\frac{\partial T'}{\partial t'} = \frac{k}{\rho C_p} \frac{\partial^2 T'}{\partial y'^2} - \frac{1}{\rho C_p} \frac{\partial q'_r}{\partial y'} \tag{2.2}$$

Conservation of species concentration:

$$\frac{\partial C'}{\partial t'} = D \frac{\partial^2 C'}{\partial y'^2} - Kr'(C' - C'_\infty) \tag{2.3}$$

Initial and boundary conditions for the fluid flow problem are given below:

$$u' = 0, T' = T'_\infty, C' = C'_\infty \text{ for all } y' \text{ and } t' \leq 0 \tag{2.4a}$$

$$u' = UH(t) \cos(\omega t'), \frac{\partial T'}{\partial y'} = -h_s T', C' = C'_w \text{ at } y' = 0 \text{ for } t' > 0 \tag{2.4b}$$

$$u' \rightarrow 0, T' \rightarrow T'_\infty, C' \rightarrow C'_\infty \text{ as } y' \rightarrow \infty \text{ for } t' > 0 \tag{2.4c}$$

where $u', g, \alpha, \rho, \beta, \beta', k, C_p, \sigma, \nu, D, T', C', Kr', q'_r$ and h_s are, respectively, the fluid velocity in the x' -direction, acceleration due to gravity, Casson fluid parameter, the fluid density, the volumetric coefficient of thermal expansion, the volumetric coefficient of expansion for concentration, thermal conductivity, specific heat at constant pressure, electrical conductivity, the kinematic viscosity, the coefficient of mass diffusivity, the temperature of the fluid, species concentration, chemical reaction parameter, radiative heat flux vector, and heat transfer coefficient.

For an optically thick fluid, in addition to emission there is also self absorption and usually the absorption co-efficient is wavelength dependent and large so we can adopt the Rosseland approximation for radiative heat flux vector q_r' . Thus q_r' is given by

$$q_r' = -\frac{4\sigma_1}{3k_1} \frac{\partial T'^4}{\partial y'} \tag{2.5}$$

where k_1 is Rosseland mean absorption co-efficient and σ_1 is Stefan-Boltzmann constant.

We assume that the temperature differences within the flow is sufficiently small, then equation (2.5) can be linearized by expanding T'^4 into Taylor's series about the free stream temperature T_∞' and neglecting second and higher order terms in $(T' - T_\infty')$. This results of the following approximations:

$$T'^4 \approx 4T_\infty'^3 T' - 3T_\infty'^4 \tag{2.6}$$

From (2.5) and (2.6) we have

$$\frac{\partial q_r'}{\partial y'} = -\frac{4\sigma_1}{3k_1} \frac{\partial^2 T'^4}{\partial y'^2} = -\frac{16\sigma_1 T_\infty'^3}{3k_1} \frac{\partial^2 T'}{\partial y'^2} \tag{2.7}$$

Thus the energy equation (2.3) reduces to

$$\frac{\partial T'}{\partial t'} = \frac{k}{\rho C_p} \frac{\partial^2 T'}{\partial y'^2} + \frac{16\sigma_1 T_\infty'^3}{3k_1 \rho C_p} \frac{\partial^2 T'}{\partial y'^2} \tag{2.8}$$

In order to reduce the governing equations (2.1), (2.3) and (2.8), into non-dimensional form, the following dimensionless variables and parameters are introduced.

$$y = \frac{y'U}{\nu}, u = \frac{u'}{U}, t = \frac{t'U^2}{\nu}, T = \frac{T' - T_\infty'}{T_w' - T_\infty'}, C = \frac{C' - C_\infty'}{C_w' - C_\infty'}, Gr = \frac{g\beta\nu T_\infty'}{U^3}, Gm = \frac{g\beta'\nu(C_w' - C_\infty')}{U^3},$$

$$Pr = \frac{\mu C_p}{k}, Sc = \frac{\nu}{D}, \gamma = \frac{h_s \nu}{U}, N = \frac{16\sigma_1 T_\infty'^3}{3kk_1}, Kr = \frac{\nu Kr'}{U^2}, \omega = \frac{\nu \omega'}{U^2}.$$

where $Gr, Gm, Pr, Sc, Kr, \gamma$ and N are, respectively, the thermal Grashof number, the solutal Grashof number, the Prandtl number, the Schmidt number, the chemical reaction parameter, Newtonian heating parameter and radiation parameter.

Equation (2.1), (2.3) and (2.8) reduces to

$$\frac{\partial u}{\partial t} = \left(1 + \frac{1}{\alpha}\right) \frac{\partial^2 u}{\partial y^2} + GrT + GmC \tag{2.9}$$

$$Pr \frac{\partial T}{\partial t} = (1 + N) \frac{\partial^2 T}{\partial y^2} \tag{2.10}$$

$$\frac{\partial C}{\partial t} = \frac{1}{Sc} \frac{\partial^2 C}{\partial y^2} - KrC \tag{2.11}$$

The corresponding initial and boundary conditions in non-dimensional form become:

$$u = 0, \theta = 0, \phi = 0 \text{ for all } y \text{ and } t \leq 0 \tag{2.12a}$$

$$u = H(t)\cos(\omega t), \frac{\partial T}{\partial y} = -\gamma(1+T), C = 1 \text{ at } y = 0 \text{ for } t > 0 \tag{2.12b}$$

$$u \rightarrow 0, T \rightarrow 0, C \rightarrow 0 \text{ as } y \rightarrow \infty \text{ for } t > 0 \tag{2.12c}$$

Here $\gamma = \frac{h_s U}{U}$ is the Newtonian heating parameter. We note that the equation (2.12b) gives $T=0$ when $\gamma = 0$, which physically means that no heating from the plate exists when $\gamma = 0$.

3 .Method of Solutions:

The set of equations (2.9), (2.10) and (2.11) subject to the initial and boundary conditions (2.12a)-(2.12c) were solved analytically using Laplace transforms. The exact solutions for fluid velocity $u(y, t)$, fluid temperature $T(y, t)$ and species concentration $C(y, t)$ are obtained and expressed in the following form:

$$\begin{aligned} u(y, t) = & \frac{H(t)}{4} e^{i\omega t} \left[e^{y\sqrt{i\omega a_1}} \operatorname{erfc} \left(\frac{y}{2} \sqrt{\frac{a_1}{t}} + \sqrt{i\omega t} \right) + e^{-y\sqrt{i\omega a_1}} \operatorname{erfc} \left(\frac{y}{2} \sqrt{\frac{a_1}{t}} - \sqrt{i\omega t} \right) \right] + \\ & \frac{H(t)}{4} e^{-i\omega t} \left[e^{y\sqrt{-i\omega a_1}} \operatorname{erfc} \left(\frac{y}{2} \sqrt{\frac{a_1}{t}} + \sqrt{-i\omega t} \right) + e^{-y\sqrt{-i\omega a_1}} \operatorname{erfc} \left(\frac{y}{2} \sqrt{\frac{a_1}{t}} - \sqrt{-i\omega t} \right) \right] + \\ & \frac{a_1 a_3}{a_2^2} \left[e^{(a_2^2 t - \gamma a_2 \sqrt{a_1})} \operatorname{erfc} \left(\frac{y}{2} \sqrt{\frac{a_1}{t}} - a_2 \sqrt{t} \right) - \operatorname{erfc} \left(\frac{y}{2} \sqrt{\frac{a_1}{t}} \right) \right] - \frac{a_1 a_3}{a_2} \left[2\sqrt{\frac{t}{\pi}} e^{-\frac{y^2 a_1}{4t}} - y\sqrt{a_1} \operatorname{erfc} \left(\frac{y}{2} \sqrt{\frac{a_1}{t}} \right) \right] - \\ & a_1 a_3 \left[\left(t + \frac{y^2 a_1}{2} \right) \operatorname{erfc} \left(\frac{y}{2} \sqrt{\frac{a_1}{t}} \right) - y\sqrt{a_1} \sqrt{\frac{t}{\pi}} e^{-\frac{y^2 a_1}{4t}} \right] - \frac{a_1 a_3}{a_2^2} \left[e^{(a_2^2 t - \gamma a_2 \sqrt{\operatorname{Pr}_{eff}})} \operatorname{erfc} \left(\frac{y}{2} \sqrt{\frac{\operatorname{Pr}_{eff}}{t}} - a_2 \sqrt{t} \right) - \operatorname{erfc} \left(\frac{y}{2} \sqrt{\frac{\operatorname{Pr}_{eff}}{t}} \right) \right] + \\ & \frac{a_1 a_3}{a_2} \left[2\sqrt{\frac{t}{\pi}} e^{-\frac{y^2 \operatorname{Pr}_{eff}}{4t}} - y\sqrt{\operatorname{Pr}_{eff}} \operatorname{erfc} \left(\frac{y}{2} \sqrt{\frac{\operatorname{Pr}_{eff}}{t}} \right) \right] + a_1 a_3 \left[\left(t + \frac{y^2 \operatorname{Pr}_{eff}}{2} \right) \operatorname{erfc} \left(\frac{y}{2} \sqrt{\frac{\operatorname{Pr}_{eff}}{t}} \right) - y\sqrt{\operatorname{Pr}_{eff}} \sqrt{\frac{t}{\pi}} e^{-\frac{y^2 \operatorname{Pr}_{eff}}{4t}} \right] + \\ & \frac{a_1 a_5}{a_6} \left[\operatorname{erfc} \left(\frac{y}{2} \sqrt{\frac{a_1}{t}} \right) - \frac{e^{-a_6 t}}{2} \left\{ e^{y\sqrt{-a_1 a_6}} \operatorname{erfc} \left(\frac{y}{2} \sqrt{\frac{a_1}{t}} + \sqrt{-a_6 t} \right) + e^{-y\sqrt{-a_1 a_6}} \operatorname{erfc} \left(\frac{y}{2} \sqrt{\frac{a_1}{t}} - \sqrt{-a_6 t} \right) \right\} \right] - \\ & \frac{a_1 a_5}{2a_6} \left[\left\{ e^{(y\sqrt{ScKr})} \operatorname{erfc} \left(\frac{y}{2} \sqrt{\frac{Sc}{t}} + \sqrt{Krt} \right) + e^{(-y\sqrt{ScKr})} \operatorname{erfc} \left(\frac{y}{2} \sqrt{\frac{Sc}{t}} - \sqrt{Krt} \right) \right\} - \right. \end{aligned}$$

$$e^{-a_6 t} \left\{ e^{(y\sqrt{Sc(Kr-a_6)})} \operatorname{erfc} \left(\frac{y}{2} \sqrt{\frac{Sc}{t}} + \sqrt{(Kr-a_6)t} \right) + e^{(-y\sqrt{Sc(Kr-a_6)})} \operatorname{erfc} \left(\frac{y}{2} \sqrt{\frac{Sc}{t}} - \sqrt{(Kr-a_6)t} \right) \right\} \quad (3.1)$$

$$T(y, t) = e^{(a_2^2 t - y a_2 \sqrt{Pr_{eff}})} \operatorname{erfc} \left(\frac{y}{2} \sqrt{\frac{Pr_{eff}}{t}} - a_2 \sqrt{t} \right) - \operatorname{erfc} \left(\frac{y}{2} \sqrt{\frac{Pr_{eff}}{t}} \right) \quad (3.2)$$

$$C(y, t) = \frac{1}{2} \left\{ e^{(y\sqrt{ScKr})} \operatorname{erfc} \left(\frac{y}{2} \sqrt{\frac{Sc}{t}} + \sqrt{Krt} \right) + e^{(-y\sqrt{ScKr})} \operatorname{erfc} \left(\frac{y}{2} \sqrt{\frac{Sc}{t}} - \sqrt{Krt} \right) \right\} \quad (3.3)$$

Note that the solution given by (3.1) is valid for $Pr_{eff} \neq a_1$. The solution for $Pr_{eff} = a_1$, can be easily obtained by substituting $Pr_{eff} = a_1$ into equation (2.10) and follow the same procedure as discussed above.

4.SKIN-FRICTION, THE RATE OF HEAT TRANSFER AND THE RATE OF MASS TRANSFER:

Skin Friction:

The expression for the skin friction at the plate for Casson fluid, is defined as

$$\begin{aligned} \tau &= - \left(1 + \frac{1}{\alpha} \right) \frac{\partial u}{\partial y} \Big|_{y=0} \\ &= \frac{1}{2a_1} \left[\sqrt{i\omega a_1} e^{i\omega t} \operatorname{erf}(\sqrt{i\omega t}) + \sqrt{-i\omega a_1} e^{-i\omega t} \operatorname{erf}(\sqrt{-i\omega t}) \right] - \frac{a_3}{a_2} (\sqrt{Pr_{eff}} - \sqrt{a_1}) \left\{ e^{a_2^2 t} (1 + \operatorname{erf}(a_2 \sqrt{t})) - 1 \right\} + \\ &2a_3 \sqrt{\frac{t}{\pi}} (\sqrt{Pr_{eff}} - \sqrt{a_1}) + \frac{1}{\sqrt{\pi t a_1}} - \frac{a_5}{a_6} \left\{ \sqrt{\frac{a_1}{\pi t}} + 2\sqrt{-a_1 a_6} e^{-a_6 t} \operatorname{erf}(\sqrt{-a_6 t}) - \sqrt{ScKr} \operatorname{erf}(\sqrt{Krt}) + \right. \\ &\left. \sqrt{Sc(Kr-a_6)} e^{-a_6 t} \operatorname{erf}(\sqrt{(Kr-a_6)t}) \right\} \end{aligned} \quad (4.1)$$

Nusselt Number:

The Nusselt number Nu, which measures the rate of heat transfer at the plate for Casson fluid is defined as

$$\begin{aligned} Nu &= - \frac{v}{U(T' - T'_\infty)} \left(\frac{\partial T'}{\partial y'} \right)_{y'=0} = \gamma \left(1 + \frac{1}{T(0, t)} \right) \\ &= a_2 \sqrt{Pr_{eff}} \left(1 + \frac{1}{e^{a_2^2 t} \left\{ 1 + \operatorname{erf}(a_2 \sqrt{t}) \right\} - 1} \right) \end{aligned} \quad (4.2)$$

Sherwood Number:

The Sherwood number Sh, which measures the rate of mass transfer at the plate, is given by

$$Sh = -\left(\frac{\partial C}{\partial y}\right)_{y=0} = \sqrt{ScKr} \operatorname{erf}(\sqrt{Krt}) + \sqrt{\frac{Sc}{\pi t}} \exp(-Krt) \quad (4.3)$$

Results and Discussions:

In order to get the physical understand of the problem and for the purpose of analyzing the effect of Casson parameter (α), Newtonian heating parameter (γ), thermal Grashof number (Gr), solutal Grashof number (Gm), Prandtl number (Pr), thermal radiation parameter (N), Schmidt number (Sc), chemical reaction parameter (Kr) and time (t) on the flow field, numerical values of the fluid velocity, fluid temperature and species concentration in the boundary layer region were computed and are displayed graphically versus boundary layer co-ordinate y in Figs 2-17. During the course of numerical calculations of the fluid velocity, the temperature and the species concentration, the values of the Prandtl number are chosen for air at $25^\circ C$ and one atmospheric pressure ($Pr=0.71$), Mercury ($Pr=0.025$), electrolytic solution ($Pr=1.0$) and water ($Pr=7.0$). To focus our attention on numerical values of the results obtained in the study, the values of Sc are chosen for the gases representing diffusing chemical species of most common interest in air, namely, hydrogen ($Sc=0.22$), water-vapour ($Sc=0.60$) and ammonia ($Sc=0.78$). To examine the effect of parameters related to the problem on the velocity field, the skin friction numerical computation are carried out at $Pr=0.71$ and $Sc=0.22$.

Figs.2-3 depicts the influence of thermal and concentration buoyancy forces on fluid velocity. It is perceived from Figs.2-3 that the fluid velocity increases close to the boundary of the wall with increasing values of Gr but it has reverse effect after attaining certain values of y whereas, it decreases on increasing value of Gm throughout the boundary layer region. Gr represents the relative strength of thermal buoyancy force to viscous force and Gm represents the relative strength of concentration buoyancy force to viscous force. Therefore, Gr decreases on decreasing the strengths of thermal buoyancy force whereas Gm decreases on decreasing the strength of concentration buoyancy force. In this problem, natural convection flow induced due to thermal and concentration buoyancy forces; therefore, thermal and concentration buoyancy force tends to decelerate the fluid velocity throughout the boundary layer region which is clearly evident from Figs.2-3.

Effect of Casson parameter α on velocity profile is clearly exhibited in Fig.4. It is observed that initially (near the wall), the fluid velocity increases (before the crossing over point) but away from the wall (after crossing over point), it decreases with increasing α . Overshoot of fluid velocity indicates that the velocity is maximum close to the surface but not at the surface. The effect of increasing values of α is to increase the fluid velocity near the wall, and hence the boundary layer thickness increases near the wall. The increasing values of the Casson parameter i.e., the decreasing yield stress (the fluid behaves as Newtonian fluid as Casson parameter becomes large i.e., for $\alpha \rightarrow \infty, \frac{1}{\alpha} \rightarrow 0$) increases the velocity field.

For different values of conjugate parameter for Newtonian heating γ , the velocity profiles are plotted in Fig..5. It is observed that initially (near the wall), the fluid velocity increases (before the crossing over point) but away from the wall (after crossing over point), it decreases with increasing γ . An increase in conjugate parameter for Newtonian heating may reduce the fluid density and increases the momentum boundary layer thickness, as a result, the velocity increases within the boundary layer.

The effect of chemical reaction Kr and thermal radiation N are shown in Figs. 6-7 respectively. From Fig.6 it is quite clear that increasing the chemical reaction parameter tends to decrease the velocity of the fluid. This means that, the chemical reaction decelerates the fluid motion. Consequently, less flow is induced along the plate resulting in decrease in the fluid velocity in the boundary layer. It should be mentioned here that physically positive values of Kr implies destructive reaction and negative values of Kr

implies generative reaction. We studied the case of a destructive chemical reaction (Kr). From Fig.7 it is observed that the fluid velocity increases with an increase in thermal radiation parameter. Physically, the higher radiation occurs when temperature is higher and hence velocity raises.

The influence of Schmidt number (Sc) on the fluid velocity and concentration profiles are depicted in Figs. 8 and.9 respectively. It is noticed from Figs.8 and .9 that, fluid velocity and concentration profiles decreases on increasing the values of Sc . The Schmidt number embodies the ratio of the momentum to the mass diffusivity. The Schmidt number therefore quantifies the relative effectiveness of momentum to mass transport by diffusion in the hydrodynamic (velocity) and concentration (species) boundary layers. As the Schmidt number increases the concentration decreases. This cause the concentration buoyancy effects to decrease yielding a reduction in the fluid velocity. The reductions in the velocity and concentration profiles are accompanied by simultaneous reductions in the velocity and concentration boundary layers. These behaviors are clear from Figs.8 and 9.

Fig. 10 shows that fluid velocity $u(y,t)$ decreases on increasing time t . This implies that, there is a reduction in fluid velocity with the progress of time throughout the thermal boundary layer region.

The velocity for different phase angle ωt is presented in Fig.11. The velocity is decreasing with increasing phase angle. The velocity close to the wall is maximum and decreasing with increasing distance from the wall, eventually tends to zero as $y \rightarrow \infty$. It is also clearly seen from this figure, that the velocity satisfies the given boundary conditions (2.12b) which provide a useful mathematical check on our calculi.

The influence of Prandtl number (Pr) on the fluid temperature is depicted in Fig. 12. It is evident from Fig. 12 that, fluid temperature θ decreases on increasing Pr . An increase in Prandtl number reduces the thermal boundary layer thickness. Prandtl number signifies the ratio of momentum diffusivity to thermal diffusivity. It can be noticed that as Pr decreases, the thickness of the thermal boundary layer becomes greater than the thickness of the velocity boundary layer according to the well-known relation $\delta T/\delta \cong 1/Pr$ where δT the thickness of the thermal boundary layer and δ the thickness of the velocity boundary layer, so the thickness of the thermal boundary layer increases as Prandtl number decreases and hence temperature profile decreases with increase in Prandtl number. In heat transfer problems, the Prandtl number controls the relative thickening of momentum and thermal boundary layers. When Prandtl number is small, it means that heat diffuses quickly compared to the velocity (momentum), which means that for liquid metals, the thickness of the thermal boundary layer is much bigger than the momentum boundary layer. Hence Prandtl number can be used to increase the rate of cooling in conducting flows.

Fig. 13 illustrates the influence of thermal radiation N on fluid temperature. It is evident from Fig. 13 that, the fluid temperature T increases on increasing N . This implies that thermal radiation tends to enhance the fluid temperature throughout the boundary layer region.

From Fig. 14 it is observed that an increase in the conjugate parameter for Newtonian heating increases the thermal boundary layer thickness and as a result the surface temperature of the plate increases. It is also observed that there is a sharp rise in temperature with the increase of conjugate parameter.

Figs.15 and 16 illustrate the influence of time on fluid temperature and species concentration respectively. It is evident from Figs. 15 and 16 that, fluid temperature and species concentration are getting accelerated with the progress of time throughout the boundary layer region. Also it may be noted that, unabated mass diffusion into the fluid stream, the molar concentration of the mixture rises with increasing time and so there is an enhancement in species concentration with the progress of time throughout the boundary layer region.

Fig.17 shows the influence of a chemical reaction on concentration profiles. In this study, we are analyzing the effects of a destructive chemical reaction ($Kr > 0$). It is noticed that concentration distributions decrease when the chemical reaction increase. Physically, for a destructive case, chemical reaction takes place with many disturbances. This, in turn, causes high molecular motion, which results in an increase in the transport phenomenon, thereby reducing the concentration distributions in the fluid flow.

FIGURES

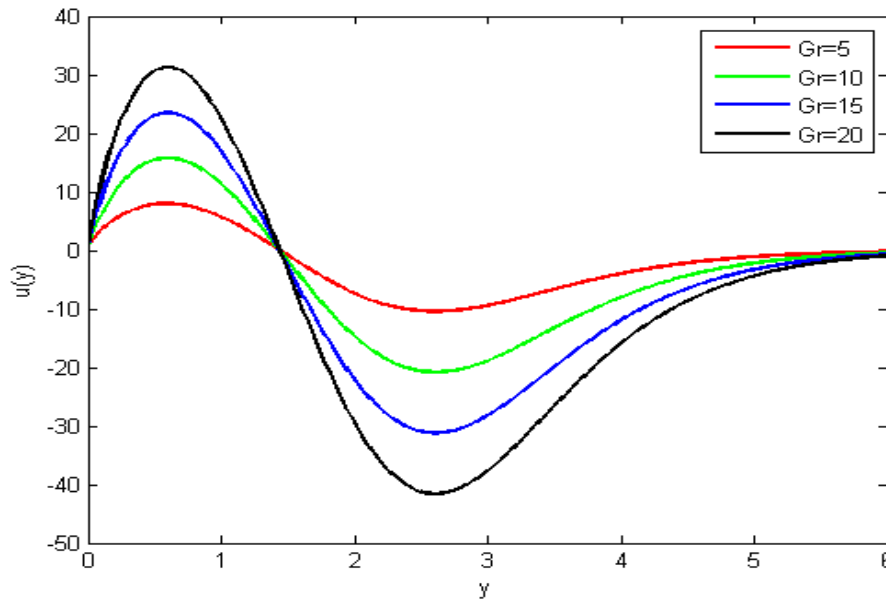


Fig.2: Velocity u against y for $Gm=5$, $Kr=1$, $Pr=0.71$, $Sc=0.22$, $\gamma=0.5$, $N=1$, $\alpha=0.5$, $t=0.7$.

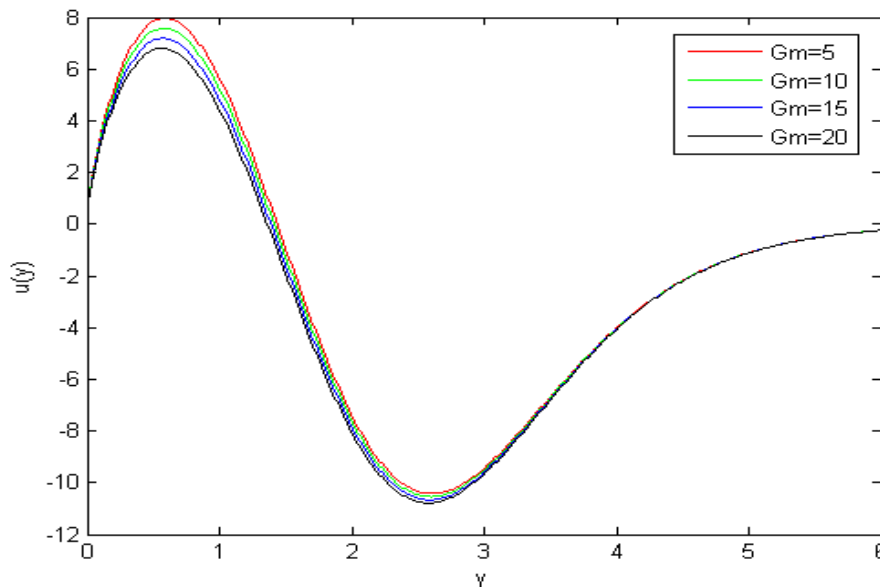


Fig 3: Velocity u against y for $Gr=5$, $Kr=1$, $Pr=0.71$, $Sc=0.22$, $\gamma=0.5$, $N=1$, $\alpha=0.5$, $t=0.7$.

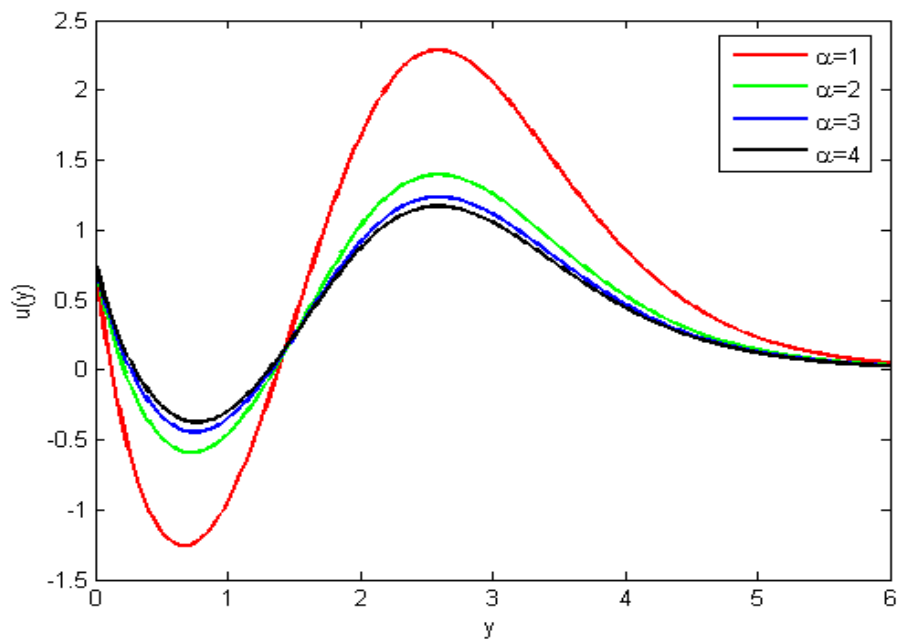


Fig.4: Velocity u against y for $Gr=5$, $Gm=5$, $Kr=1$, $Pr=0.71$, $Sc=0.22$, $\gamma=0.5$, $N=1$, $t=0.7$.

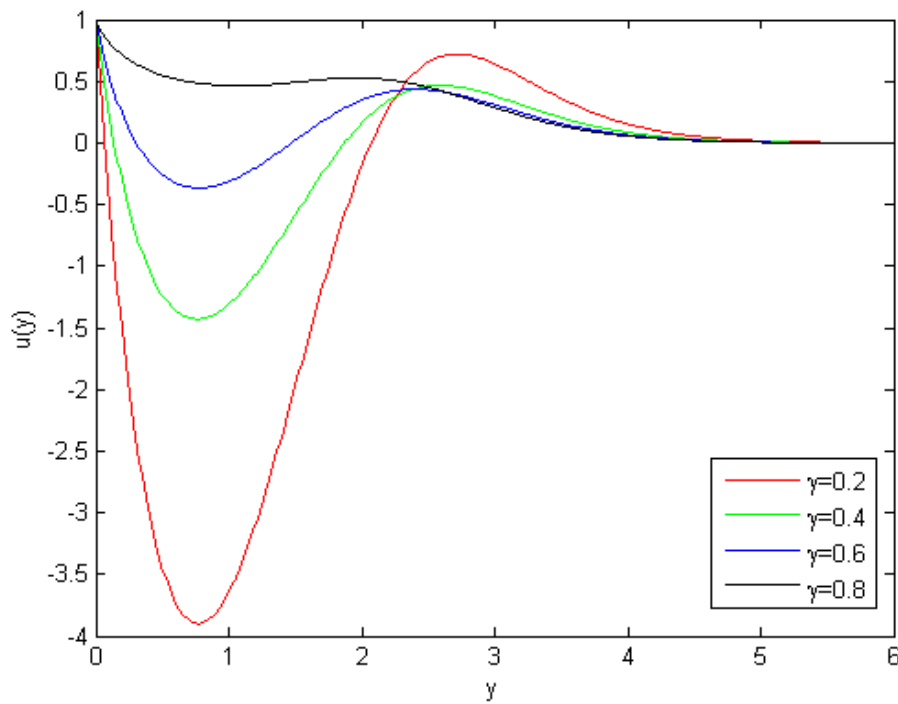


Fig.5: Velocity u against y for $Gr=5$, $Gm=5$, $Kr=1$, $Pr=0.71$, $Sc=0.22$, $N=1$, $\alpha=0.5$, $t=0.7$.

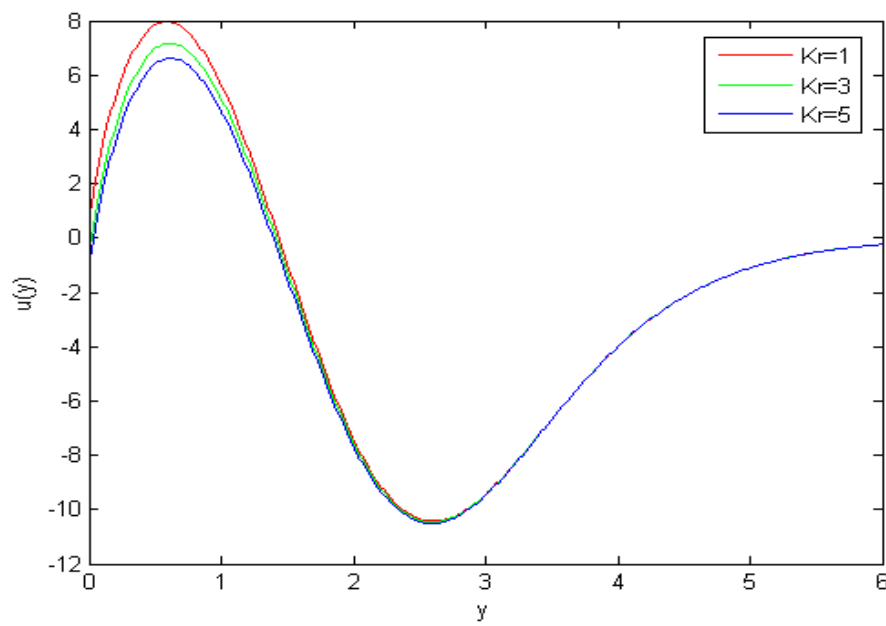


Fig.6: Velocity u against y for $Gr=5$, $Gm=5$, $Pr=0.71$, $Sc=0.22$, $\gamma=0.5$, $N=1$, $\alpha=0.5$, $t=0.7$.

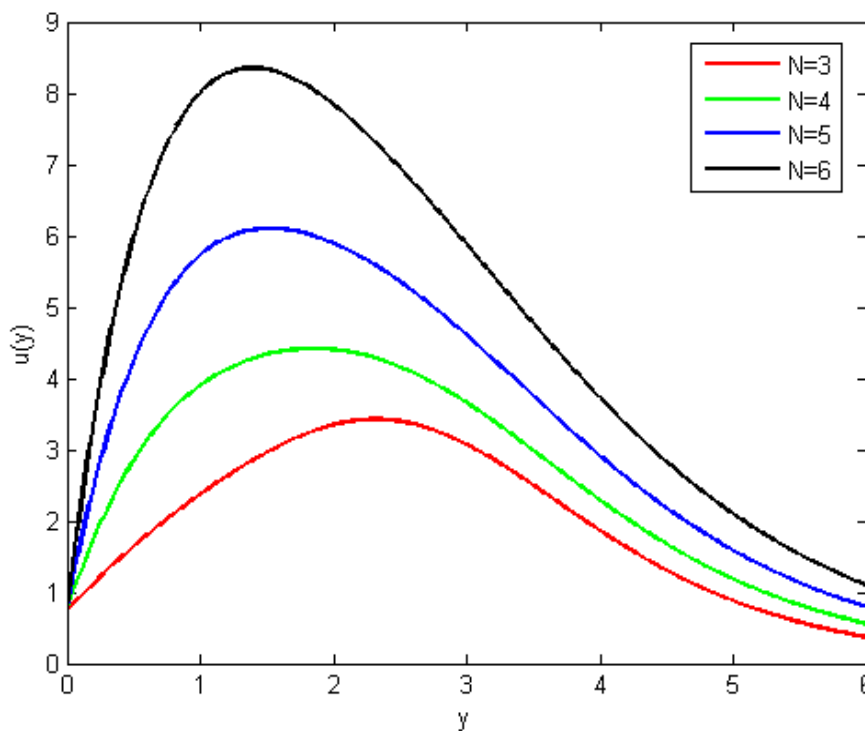


Fig.7: Velocity u against y for $Gr=5$, $Gm=5$, $Kr=1$, $Pr=0.71$, $Sc=0.22$, $\gamma=0.5$, $\alpha=0.5$, $t=0.7$.

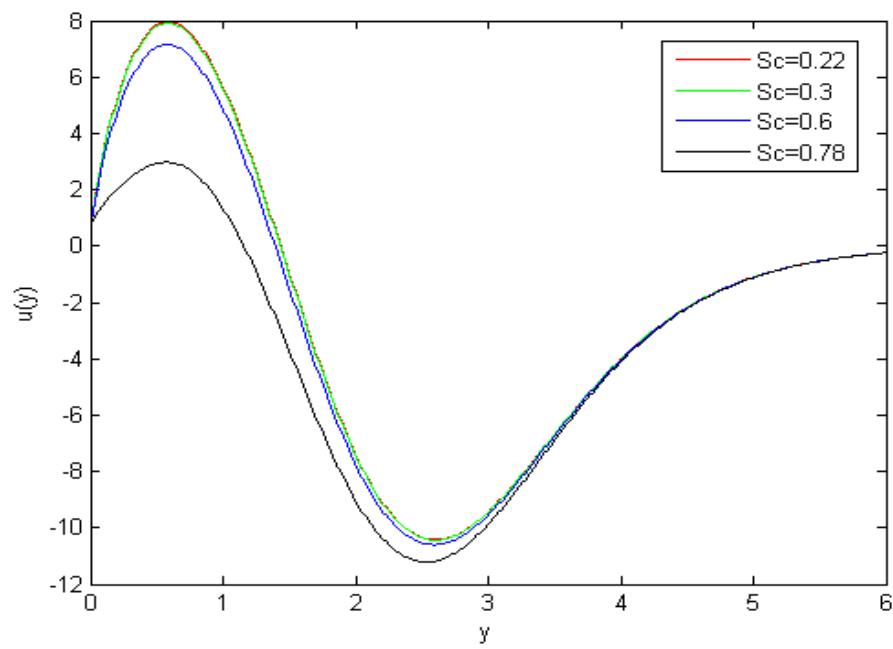


Fig.8: Velocity u against y for $Gr=5$, $Gm=5$, $Kr=1$, $Pr=0.71$, $\gamma=0.5$, $N=1$, $\alpha=0.5$, $t=0.7$.

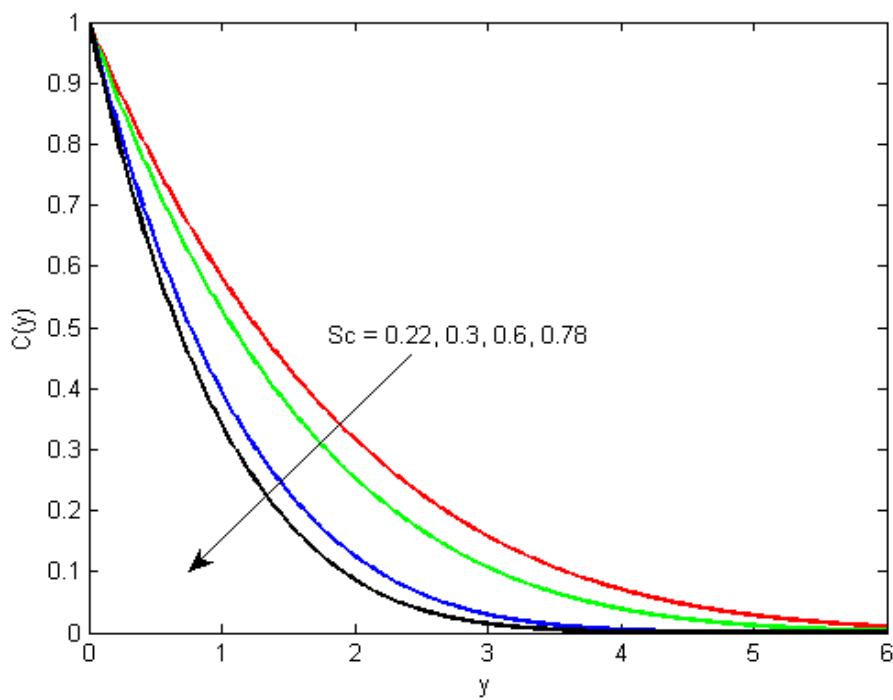


Fig..9: Concentration C against y for $Kr=1$, $t=0.7$.

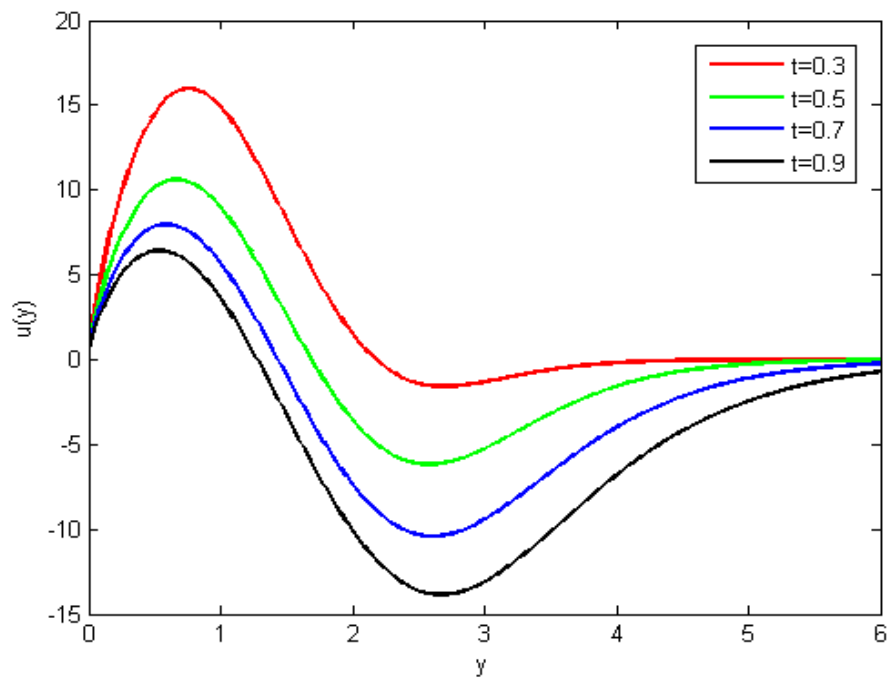


Fig.10: Velocity u against y for $Gr=5$, $Gm=5$, $Kr=1$, $Pr=0.71$, $Sc=0.22$, $\gamma=0.5$, $N=1$, $\alpha=0.5$.

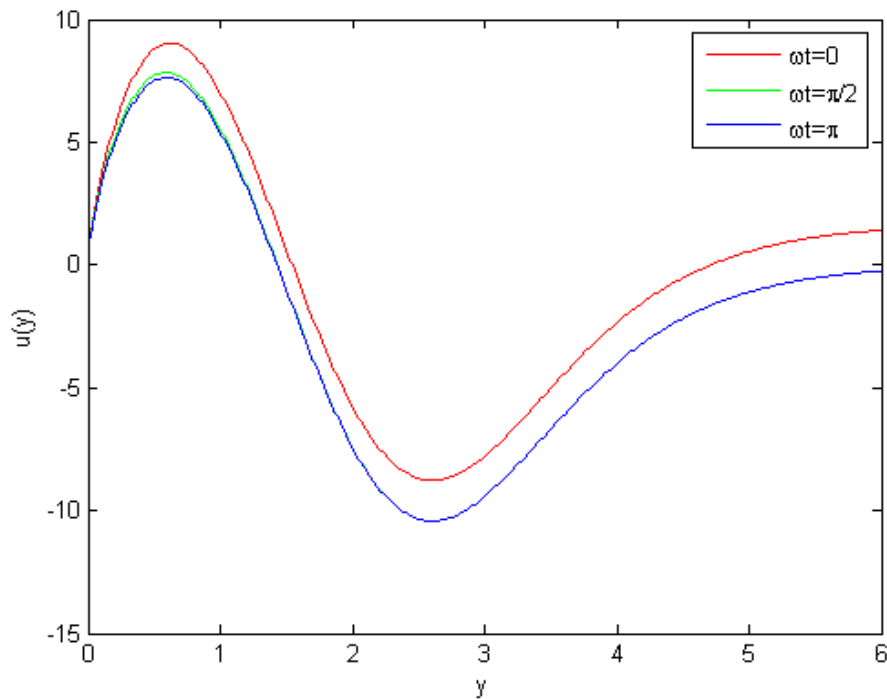


Fig.11: Velocity u against y for $Gr=5$, $Gm=5$, $Kr=1$, $Pr=0.71$, $Sc=0.22$, $\gamma=0.5$, $N=1$, $\alpha=0.5$, $t=0.7$.

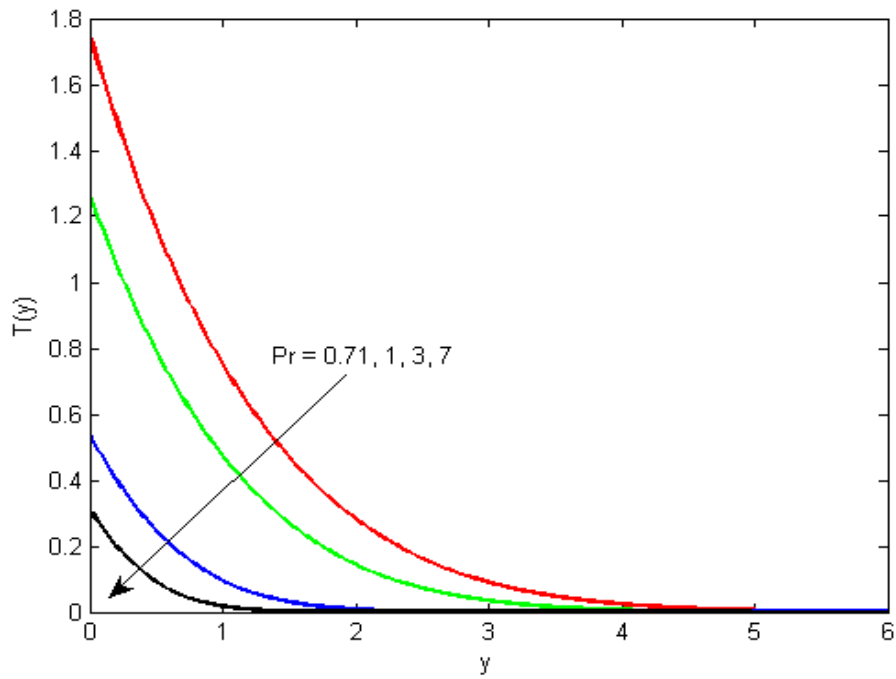


Fig.12: Temperature T against y for $\gamma=0.5$, $N=1$, $t=0.7$.

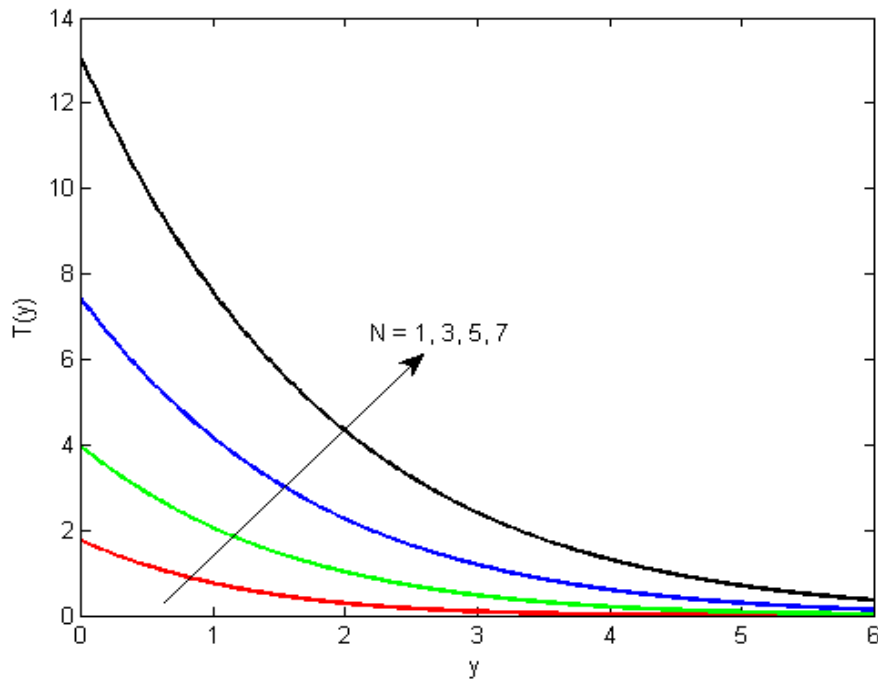


Fig.13: Temperature T against y for $Pr=0.71$, $\gamma=0.5$, $t=0.7$.

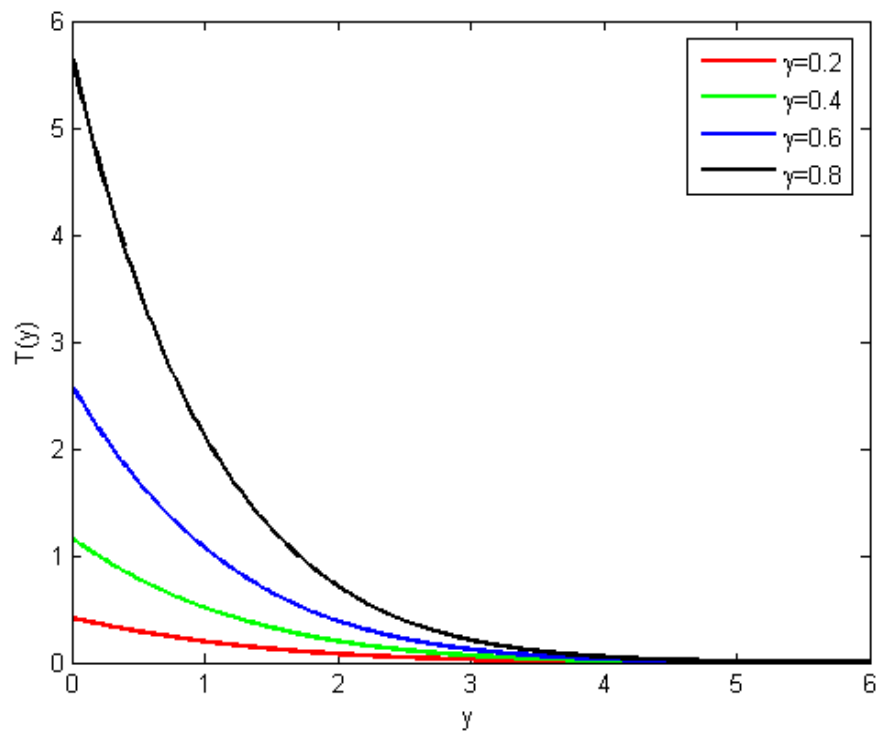


Fig.14: Temperature T against y for $Pr=0.71, N=1, t=0.7$.

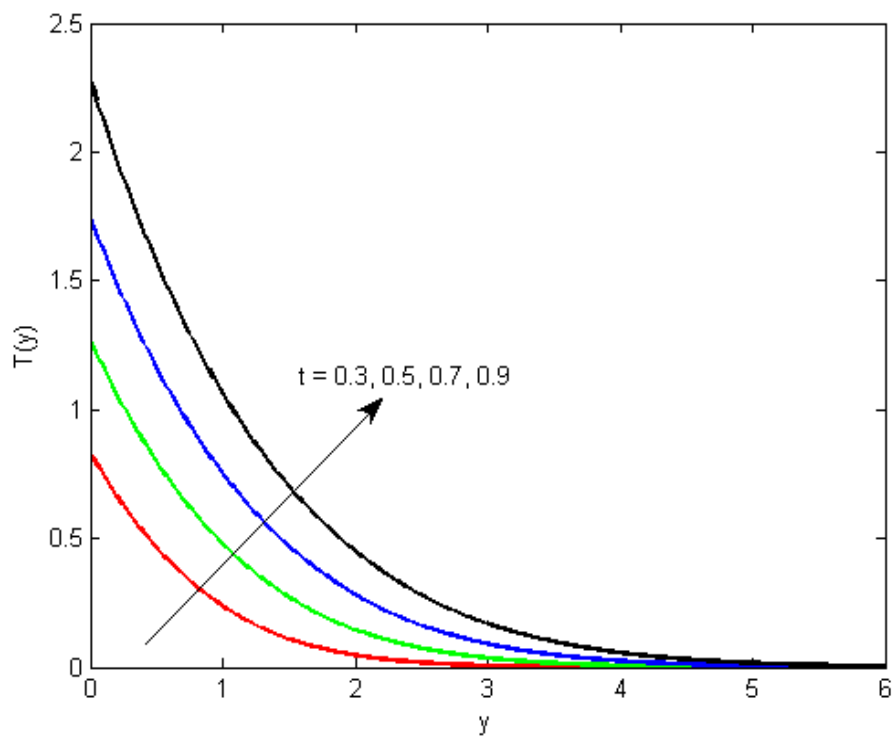


Fig.15: Temperature T against y for $Pr=0.71, \gamma=0.5, N=1$.

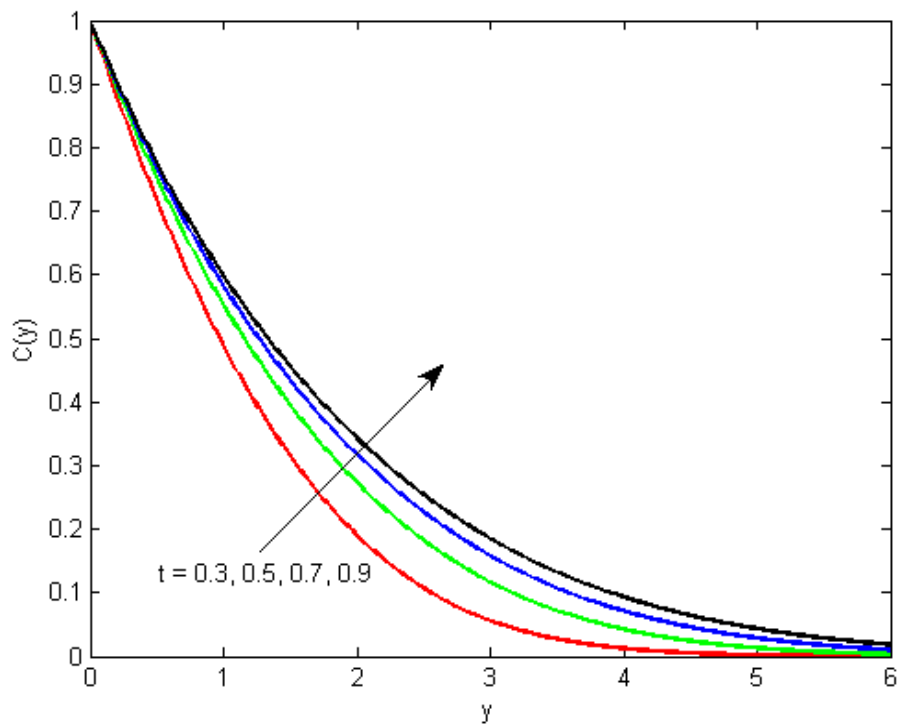


Fig.16: Concentration C against y for $Sc=0.22$, $Kr=1$.

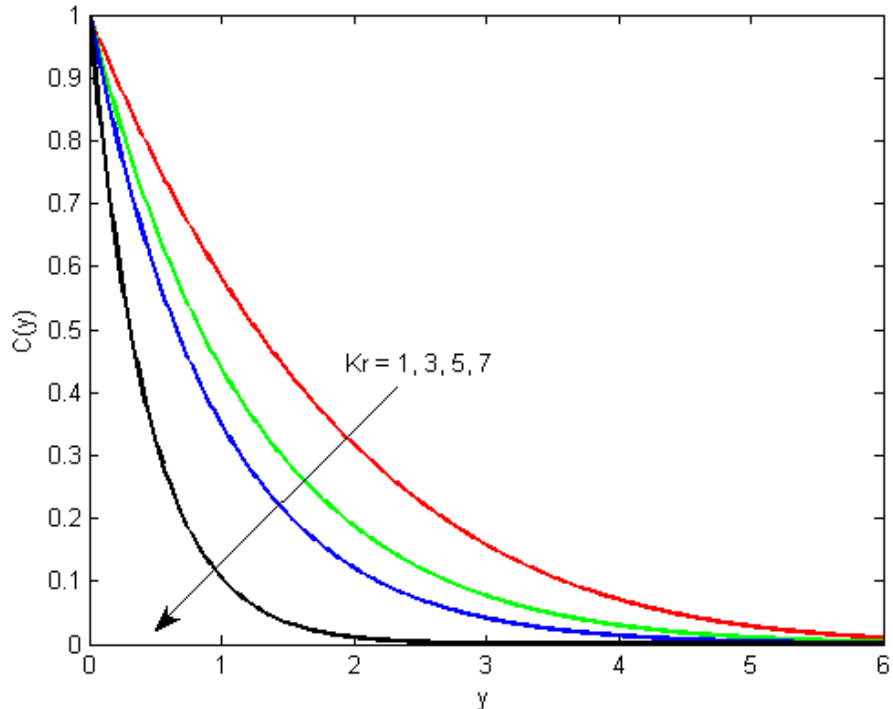


Fig.17: Concentration C against y for $Sc=0.22$, $t=0.7$.

REFERENCES

- [1] Vajervelue K. and Shastri K.S. (1980): “Natural convection heat transfer in vertical wavy channels”, Int. J. Heat Mass Transfer, Vol.23, pp.408-411.
- [2] Rajsekhar K., Raman Reddy G.V. and Prasad B.D.C.N. (2012): “Unsteady MHD free convective flow past a semi-infinite vertical porous plate”, Int. J. of Modern Eng. Research, Vol.2, No.5, pp.3123-3127.
- [3] Jefferey G.B. (1915): “The two dimensional steady motion of a viscous fluid”, Phil. Mag., Vol.29, pp.455-465.
- [4] Lekoudis S.G., Nayfeh A.H. and Sarie W.S. (1976): “Compressible boundary layers over wavy walls”, Phys. of Fluids, Vol.19, pp.514-519.
- [5] Vajervelue K. and Shastri K.S. (1978): “Free convective heat transfer problems between a long vertical wavy wall and a parallel flat wall”, J. Fluid Mech., Vol.86, pp.365.
- [6] Shankar P.N. and Sinha U.N. (1976): “The Rayleigh problem for a wavy wall”, J. Fluid Mech., Vol.77, pp.243-256.
- [7] Lesson M. and Gangwati S.T. (1976): “Effect of small amplitude wall waviness upon the stability of the boundary layers”, Phys. Fluids, Vol.19, pp.510-513.
- [8] Rao C.N.B. and Sastri K.S. (1982): “The response of skin friction, wall heat transfer and pressure drop to wall waviness in the presence of buoyancy”, Indian J. Maths and Math. Sci., Vol.5, No.3, pp.585-594.
- [9] Ahmadi G. and Mani R, (1971): “Equation of motion for a viscous flow through a rigid porous medium”, Indian J. Tech., Vol.9, pp.441-452.
- [10] Rucha Luiz: “Convection in channels and porous media”, VDM Verlag.
- [11] Kundu K.P. and Cohen M.I.: “Fluid Mechanics”, Academic Press.
- [12] Schaaf S.A. and Chambre P.L. (1961): “Flow of,”, Princeton Press.
- [13] Yamamoto K. and Lwamura N. (1976): “Flow with convective acceleration through a porous medium”, J. Eng. Math, Vol.10, pp.41-54.
- [14] Zarrouk S.J.: “Reacting flows in porous media”, VDM Verlag.
